

# ChemistrySelect

Supporting Information

## **Dense MoS<sub>2</sub> Micro-Flowers Planting on Biomass-Derived Carbon Fiber Network for Multifunctional Sulfur Cathodes**

Rameez Razaq, Nana Zhang, Ying Xin, Qian Li, Jin Wang, and Zhaoliang Zhang\*

## **Experimental Section**

### **Preparation of MoS<sub>2</sub>/CFs composites**

Commercial tissue paper (TP) was employed as a biomass source of carbon. TP was first purified by soaking in 1 mol L<sup>-1</sup> HCl solution (20 mL) for 24 h and then washed several times with deionized (DI) water by vacuum filtration followed by drying at 80 °C overnight before further use. To grow MoS<sub>2</sub> flowers on TP, ammonium molybdate tetrahydrate (76.7 mg) and thiourea (1 g) was first dissolved in 20 mL DI water. Then, purified TP (76.7 mg) was immersed in above solution. After hydrothermal treatment at 180 °C for 24 h, the suspension was filtrated and washed with DI water several times and dried at 80 °C overnight followed by calcination at 800 °C under Ar atmosphere for 2 h. The as-prepared sample was named as MoS<sub>2</sub>/CFs. As a control sample, CFs was prepared from commercial TP in a similar procedure except for a hydrothermal treatment.

### **Formation of S-MoS<sub>2</sub>/CFs (S-CFs) composites**

The S-MoS<sub>2</sub>/CFs (S-CFs) composite was prepared by the vapour infusion method. Briefly, sulfur powder and MoS<sub>2</sub>/CFs (CFs) were thoroughly mixed and then sealed in a glass vial under Ar atmosphere. After heat-treatment at 300 °C for 4 h and cooling down to room temperature, the S-MoS<sub>2</sub>/CFs (S-CFs) composite was obtained.

### **Structural characterizations**

X-ray diffraction (XRD) patterns were recorded on a D8 FOCUS powder X-ray diffraction instrument (Burker AXS, Germany) using 40 Kv as tube voltage and 40 mA as tube current. Field emission scanning electron microscopy (FESEM)

equipped with energy dispersive spectroscopy (EDS) was performed on a Hitachi SU-70 microscope. Transmission electron microscopy (TEM) was conducted on a JEOL JEM-2010 microscope at an accelerating voltage of 200 kV. X-ray photoelectron spectroscopy (XPS) data were obtained on thermo scientific ESCALAB 250 XI electron spectrometer, using monochromatic Al K $\alpha$  as exciting radiation at constant passing energy of 1486.6 eV. Thermo-gravimetry analysis (TGA) was conducted on NETZSCH, STA449 from room temperature to 800 °C with a heating rate of 10 K min<sup>-1</sup> in Ar.

### **Preparation of sulfur electrodes and electrochemical measurement**

Sulfur electrodes were prepared by mixing 80% S-MoS<sub>2</sub>/CFs (S-CFs), 10% super P and 10% poly (vinylidene fluoride) (PVDF, Sigma-Aldrich) binder in *N*-methyl 2-pyrrolidone (NMP, Sigma-Aldrich) solvent. Typically, 80% S-MoS<sub>2</sub>/CFs (CFs) and 10% super P were mixed in a mortar by hands for a certain time followed by adding 10% PVDF binder and NMP solvent to form a slurry. The slurry was then pasted on aluminum foil with the active material thickness of ~1.5 and 4.2 mg cm<sup>-2</sup> and then dried at 60 °C for 12 hours. To measure the electrochemical properties, 2025-type stainless steel coin cells were assembled inside an Ar-filled glovebox with lithium as the anode and a polypropylene (PP) film (Celgard 2400) as the separator. The electrolyte was prepared by dissolving lithium bis trifluoromethanesulphonylimide (LITFSI, 99%, Acros Organics, 1 M) and lithium nitrate (LiNO<sub>3</sub>, 99.9%, Alfa Aesar, 0.1 M) in 1,2-dimethoxyethane (DME, 99.5%, Alfa Aesar) and 1,3-dioxolane (DOL, 99.5%, Alfa Aesar) (1:1 ratio, by volume). Typically, the electrolyte/sulfur ratio was about ~14  $\mu$ L per mg sulfur. The electrolyte was added on the center of the cathode by using micropipette. A

LAND galvanostatic charge/discharge system was used. Stepwise rate performance was inspected at current rates of 0.2 C, 0.5 C, 1 C, 2 C, and 4 C. The charge/ discharge voltage range was 1.7-2.8 V. The CV tests were performed at a scan rate of 0.1, 0.2, 0.3, and 0.4 mV s<sup>-1</sup> on an electrochemical workstation (SP-300, Bio-logic). Electrochemical impedance spectroscopy (EIS) measurements were conducted at a frequency range of 100 kHz to 100 mHz on SP-300.

### **Symmetrical cell assembly and measurements**

Either MoS<sub>2</sub>/CFs (or CFs) and PVDF binder at a 3:1 weight ratio were dispersed in NMP. The slurry was stirred well and pasted on aluminum foil with successive heating at 60 °C for 12 h. After drying, the electrode disks with a diameter of 12 mm were punched out and employed as working and reference electrodes. For the assembly of symmetrical cells, 40 μL of the electrolyte containing 0.5 mol L<sup>-1</sup> Li<sub>2</sub>S<sub>6</sub> and 1 mol L<sup>-1</sup> LiTFSI in tetraglyme was used. The cyclic voltammetry (CV) tests were performed on SP-300 at a scan rate of 50 mV s<sup>-1</sup>. EIS measurements of symmetrical cells were performed at a frequency range of 100 kHz to 100 mHz on SP-300.

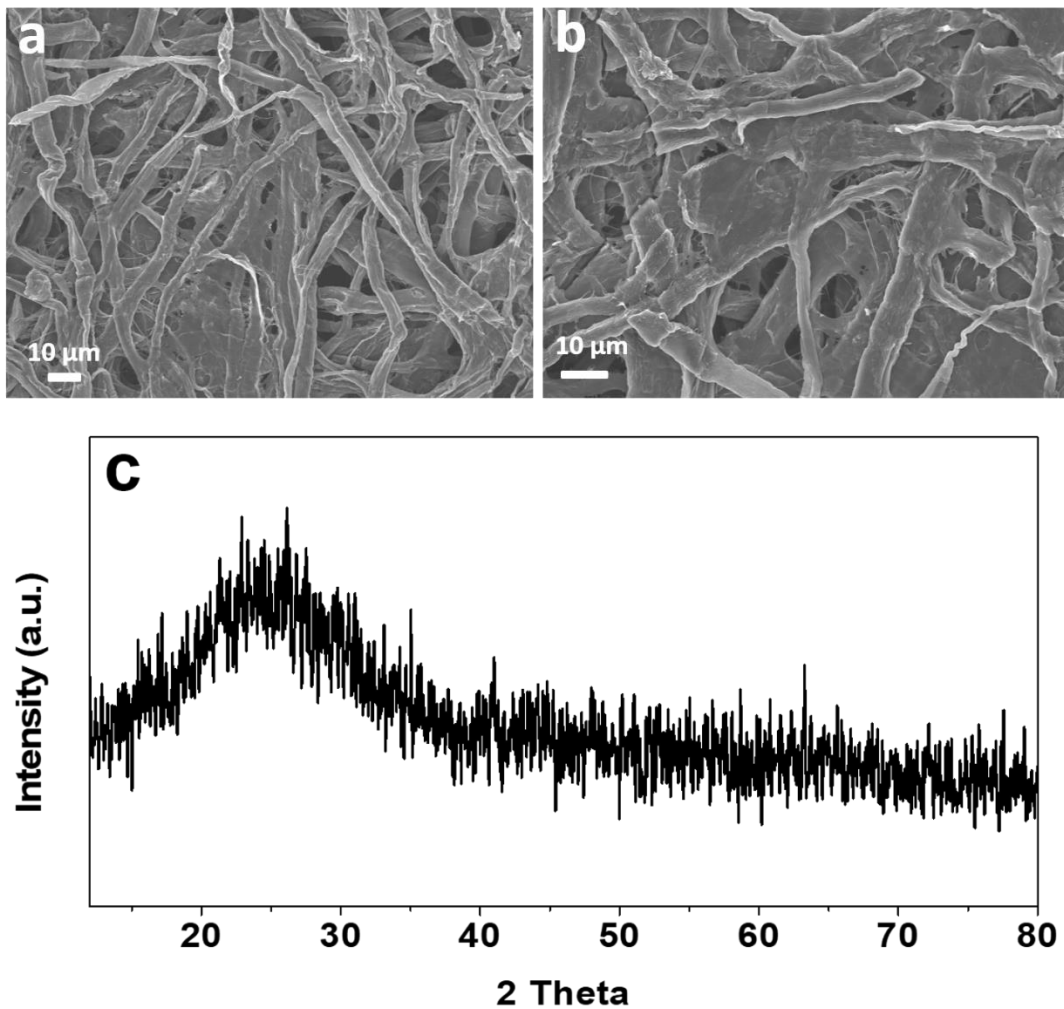


**Fig. S1.** FESEM images (a, b) and XRD (c) of tissue paper derived CFs.

In Fig. S1, one broad peak at  $2\theta$  of  $24^\circ$  and the other negligible peak at  $44^\circ$  were attributed to the (002) and (101) diffraction planes of carbon, respectively.

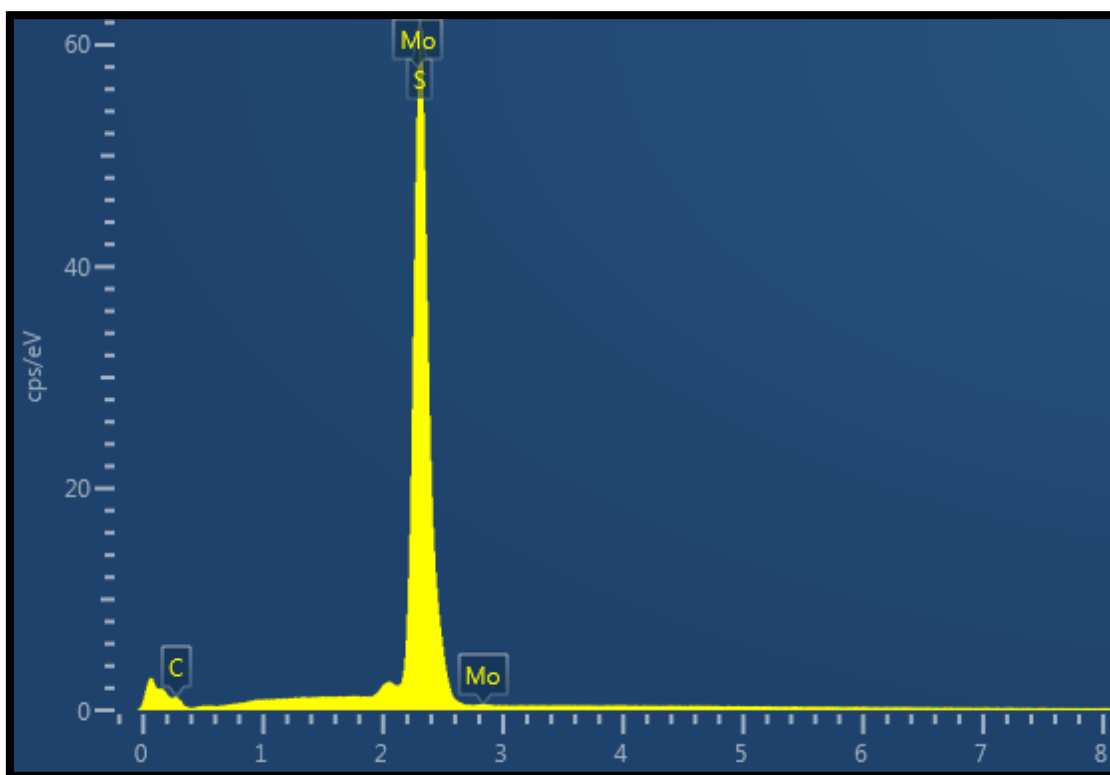


**Fig. S2.** EDS spectra of MoS<sub>2</sub>/CFs.

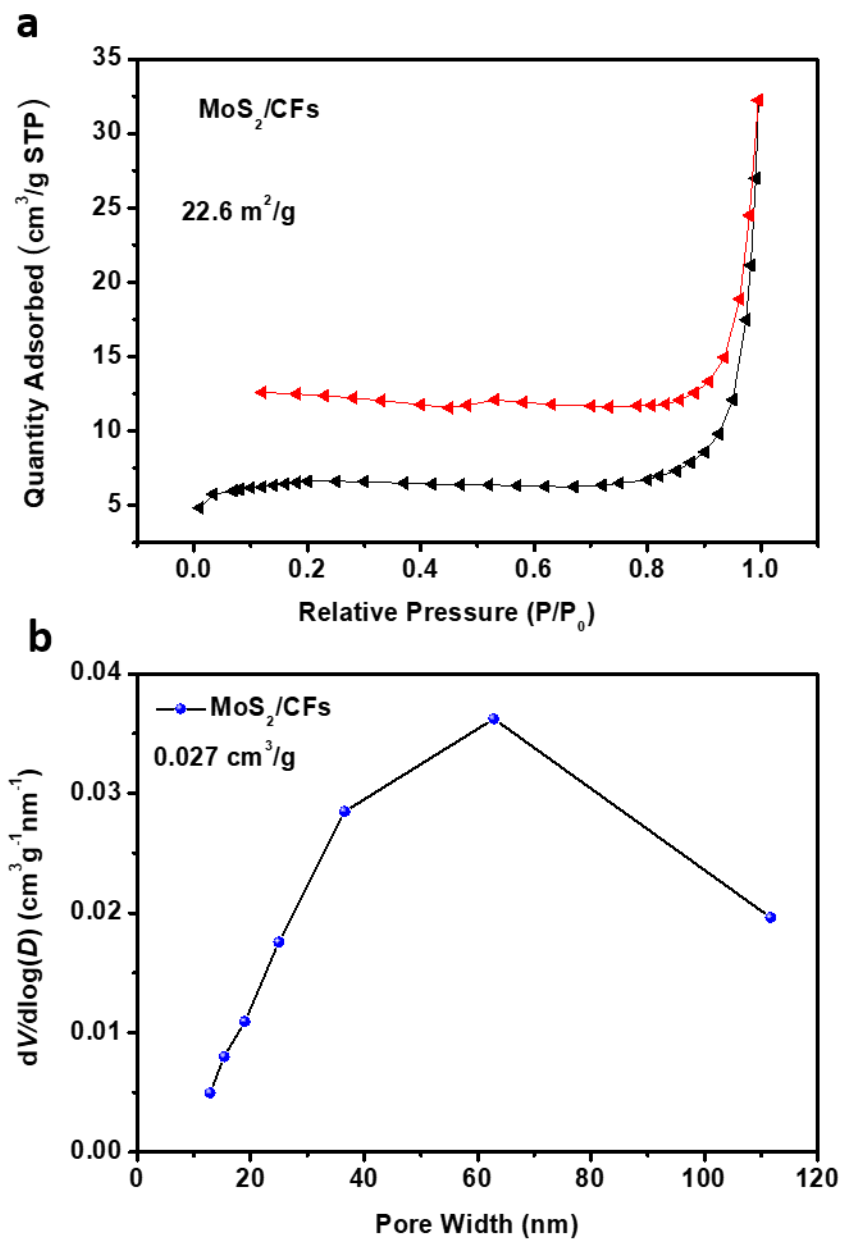


**Fig. S3.** N<sub>2</sub> adsorption/desorption isotherm (a) and pore size distribution (b) of MoS<sub>2</sub>/CFs.

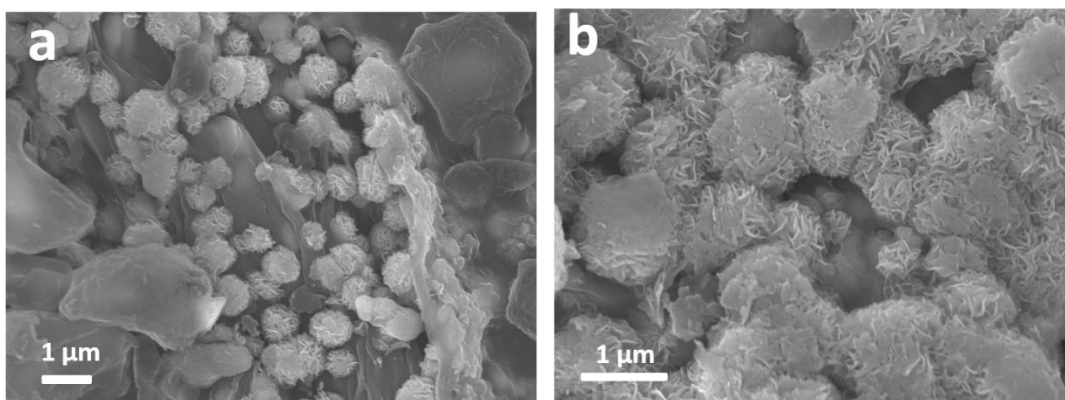


**Fig. S4.** FESEM images of S-MoS<sub>2</sub>/CFs by melt diffusion method (a), and *in situ* oxidation method (b).



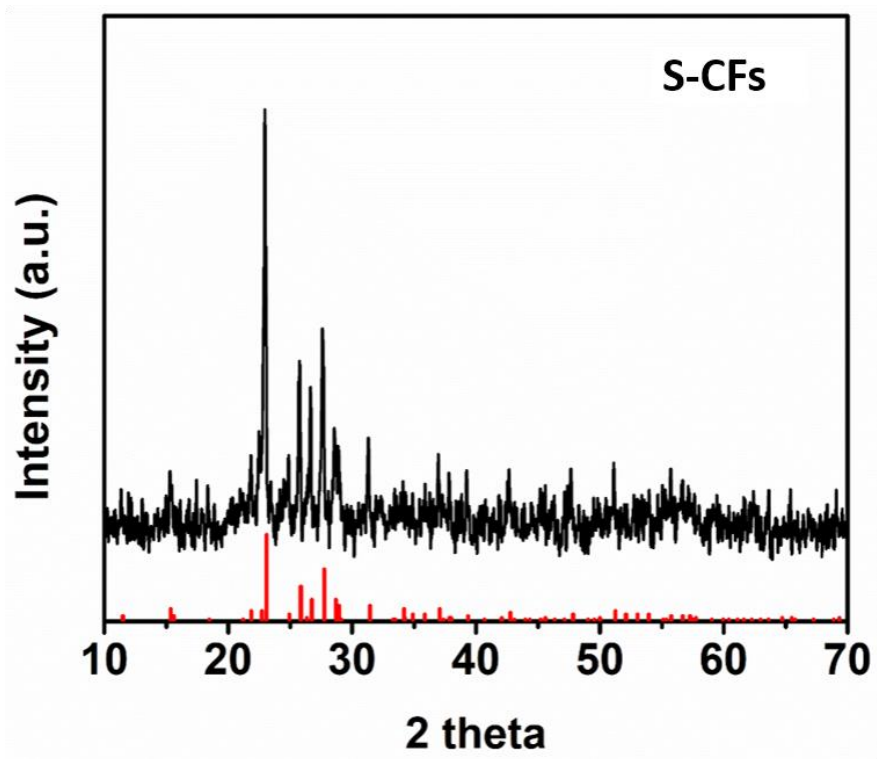


Fig. S5. XRD pattern of S-CFs.

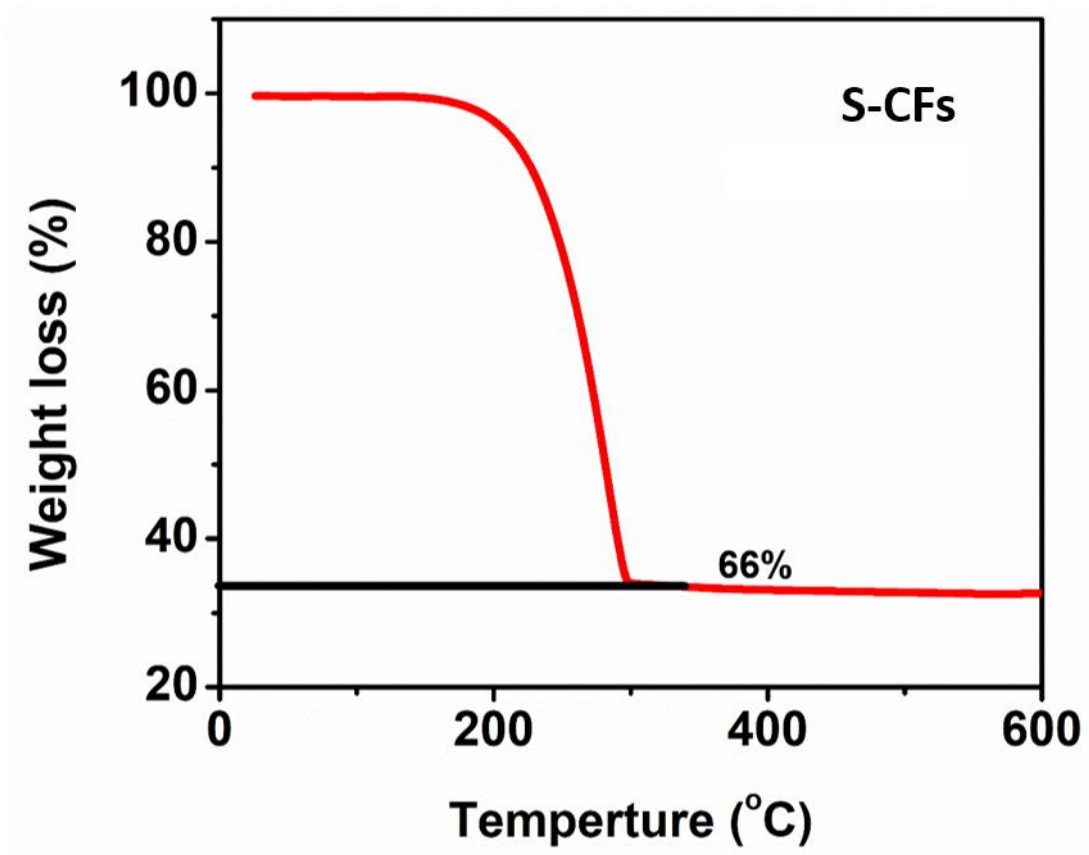


Fig. S6. TGA profile of S-CFs.

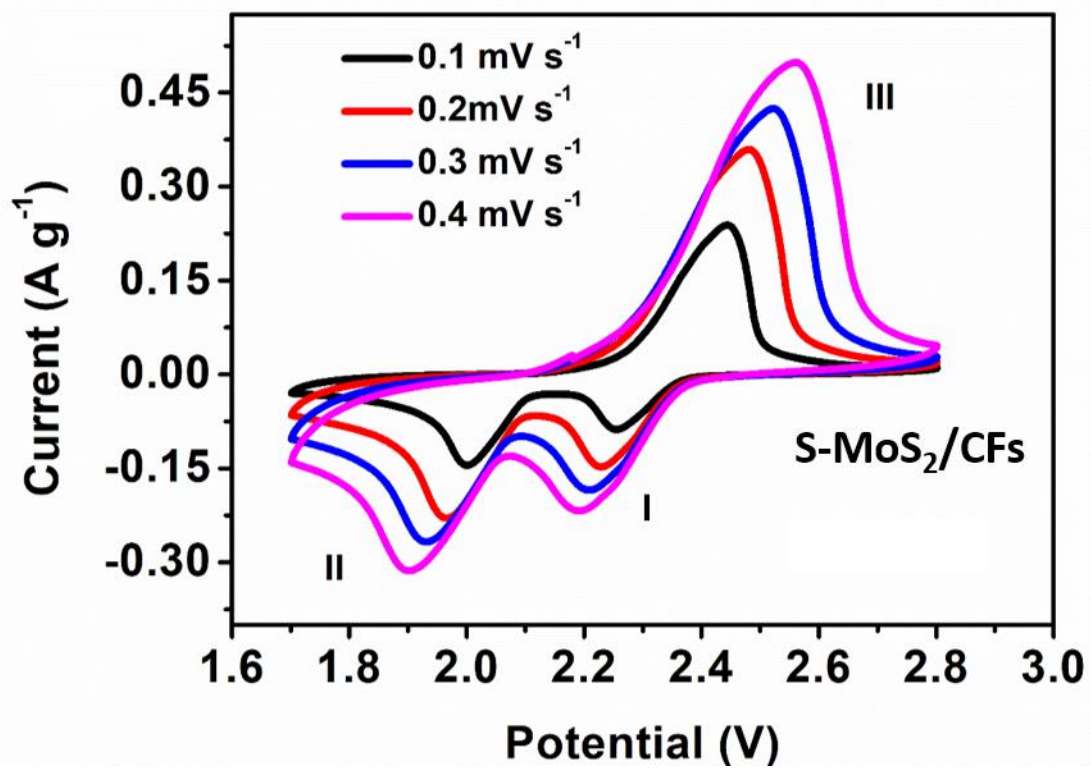


Fig. S7. CV profiles of S-MoS<sub>2</sub>/CFs at different scan rates.

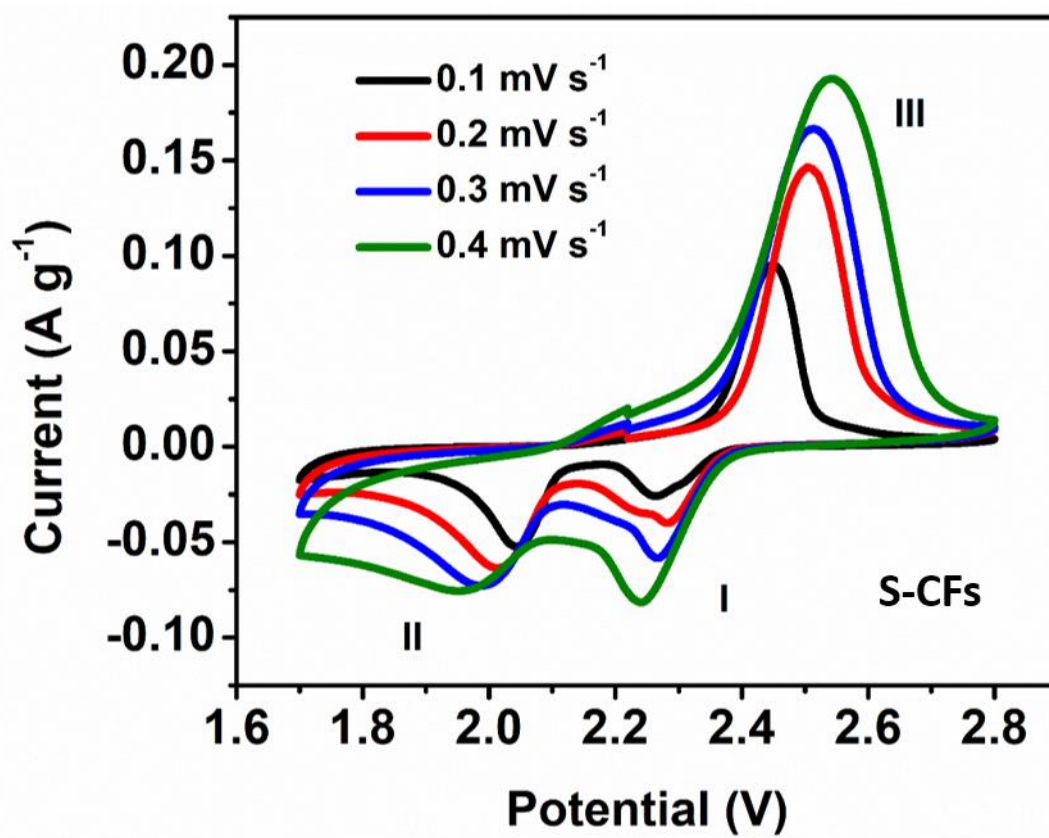


Fig. S8. CV profiles of S-CFs at different scan rates.

**Table S1.** Comparison of the electrochemical performance of this work with previously reported literatures related to LSBs.

| Cathode material             | Initial Capacity mAh g <sup>-1</sup> | Capacity retention mAh g <sup>-1</sup> | C-rate     | Capacity retention % | Coulombic efficiency % | References       |
|------------------------------|--------------------------------------|--|------------|----------------------|------------------------|------------------|
| S-<br>VS <sub>2</sub> @G/CNT | 830                                  | 701                                    | 0.5        | 84                   | 99.5                   | [1]              |
| S/GN-CNT                     | 758                                  | 463                                    | 0.5        | 61                   | N.A                    | [2]              |
| S@Co-<br>NCNT/NP             | 908                                  | 657                                    | 0.5        | 72                   | >99                    | [3]              |
| POF-HS/S                     | 955                                  | 773                                    | 0.5        | 80                   | >99                    | [4]              |
| TiO@C-HS/S                   | 1066                                 | 630                                    | 0.5        | 59                   | >99                    | [5]              |
| TiN-S                        | 988                                  | 644                                    | 0.5        | 65                   | >98                    | [6]              |
| S-Co <sub>4</sub> N/NG       | 1109                                 | 776                                    | 0.5        | 70                   | 95                     | [7]              |
| S-Ni <sub>3</sub> FeN/G      | 900                                  | 801                                    | 0.5        | 89                   | >98                    | [8]              |
| <b>S-MoS<sub>2</sub>/CFs</b> | <b>1033</b>                          | <b>912</b>                             | <b>0.5</b> | <b>88</b>            | <b>&gt;99</b>          | <b>This work</b> |
| <b>S-MoS<sub>2</sub>/CFs</b> | <b>714</b>                           | <b>533</b>                             | <b>2</b>   | <b>75</b>            | <b>&gt;99</b>          | <b>This work</b> |

## References

- [1] G. Zhou, H. Tian, Y. Jin, X. Tao, B. Liu, R. Zhang, Z. W. Seh, D. Zhuo, Y. Liu, J. Sun, J. Zhao, C. Zu, D. S. Wu, Q. Zhang, Y. Cui, *Proc. Natl. Acad. Sci. U. S. A.* **2017**, *114*, 840.
- [2] Z. Zhang, L.-L. Kong, S. Liu, G.-R. Li, X.-P. Gao, *Adv. Energy Mater.* **2017**, *7*, 1602543.
- [3] T. Chen, B. Cheng, G. Zhu, R. Chen, Y. Hu, L. Ma, H. Lv, Y. Wang, J. Liang, Z. Tie, Z. Jin, J. Liu, *Nano Lett.* **2017**, *17*, 437.
- [4] B. Q. Li, S. Y. Zhang, L. Kong, H. J. Peng, Q. Zhang, *Adv. Mater.* **2018**, *30*, e1707483.
- [5] Z. Li, J. Zhang, B. Guan, D. Wang, L.-M. Liu, X. W. Lou, *Nat. Commun.* **2016**, *7*, 13065.
- [6] Z. Cui, C. Zu, W. Zhou, A. Manthiram, J. B. Goodenough, *Adv. Mater.* **2016**, *28*, 6926.
- [7] M. Zhao, H. J. Peng, B. Q. Li, X. Chen, J. Xie, X. Liu, Q. Zhang, J. Q. Huang, *Angew. Chem. Int. Ed.* **2020**, *59*, 9011.
- [8] M. Zhao, H. J. Peng, Z. W. Zhang, B. Q. Li, X. Chen, J. Xie, X. Chen, J. Y. Wei, Q. Zhang, J. Q. Huang, *Angew. Chem. Int. Ed.* **2019**, *58*, 3779.